Cell, Vol. 106, 453–463, August 24, 2001, Copyright ©2001 by Cell Press

Translocation of σ^{70} with RNA Polymerase during Transcription: Fluorescence Resonance Energy Transfer Assay for Movement Relative to DNA

Jayanta Mukhopadhyay,[2] Achillefs N. Kapanidis,[2,3] Vladimir Mekler, Ekaterine Kortkhonjia, Yon W. Ebright, and Richard H. Ebright[1]
Howard Hughes Medical Institute
Waksman Institute
Department of Chemistry
Rutgers University
Piscataway, New Jersey 08854

Summary

Using fluorescence resonance energy transfer, we show that, in the majority of transcription complexes, σ^{70} is not released from RNA polymerase upon transition from initiation to elongation, but, instead, remains associated with RNA polymerase and translocates with RNA polymerase. The results argue against the presumption that there are necessary subunit-composition differences, and corresponding necessary mechanistic differences, in initiation and elongation. The methods of this report should be generalizable to monitor movement of any molecule relative to any nucleic acid.

Introduction

σ^{70} interacts with *Escherichia coli* RNA polymerase (RNAP) to yield RNAP holoenzyme (Gross et al., 1998). σ^{70} contains determinants for sequence-specific interaction with promoter DNA and, through these determinants, targets RNAP holoenzyme to promoters. σ^{70} also orchestrates events in transcription initiation.

It generally is believed that σ^{70} is released from RNAP at the transition from transcription initiation to elongation—i.e., upon synthesis of an RNA product of a critical threshold length of 9–11 nt (Travers and Burgess, 1969; Hansen and McClure, 1980; Straney and Crothers, 1985; Krummel and Chamberlin, 1989; Metzger et al., 1993). Thus, it generally is believed that a "σ cycle" exists, with association of σ^{70} with RNAP to permit initiation, and dissociation of σ^{70} from RNAP to permit elongation (Travers and Burgess, 1969; Hansen and McClure, 1980; Straney and Crothers, 1985; Krummel and Chamberlin, 1989; Metzger et al., 1993). Furthermore, it generally is believed, based on this presumed difference in subunit composition of the transcription machinery in transcription initiation and elongation, that there is a fundamental mechanistic difference in transcription initiation and elongation (Carpousis and Gralla, 1985; Straney and Crothers, 1987; Krummel and Chamberlin, 1989; Metzger et al., 1993).

The belief that σ^{70} is released from RNAP at the transition from transcription initiation to elongation is based on the observation that σ^{70} is present in chromatographically or electrophoretically isolated RNAP-promoter open complexes (RP_o), but is not present in chromatographically or electrophoretically isolated RNAP-DNA elongation complexes (RD_e)—including RNAP-DNA elongation complexes with RNA products as short as 9–11 nt ($RD_{e,9}$, $RD_{e,10}$, and $RD_{e,11}$) (Hansen and McClure, 1980; Straney and Crothers, 1985; Krummel and Chamberlin, 1989; Metzger et al., 1993). However, this observation is not definitive. The experiments involved a harsh separative step (chromatography or electrophoresis) that could transform a difference in stability of interactions of σ^{70} with the remainder of the complex in RP_o and RD_e into an artifactual difference in occupancy of σ^{70} in RP_o and RD_e. Thus, an alternative model also must be considered: a model in which stability of interactions of σ^{70} with the remainder of the complex is reduced at the transition to elongation—e.g., due to unfavorable interactions between nascent RNA and σ^{70} (Daube and von Hippel, 1999)—but in which σ^{70} is not released at the transition to elongation.

Several observations have challenged the σ^{70}-release model (Shimamoto et al., 1986; Osumi-Davis et al., 1987; Ring et al., 1996). Most notably, it has been observed that σ^{70} is involved in pausing in the +16/+17 region of λ $P_{R'}$, recognizing a sequence element in the transcribed region of λ $P_{R'}$ (Ring et al., 1996). However, previously, there has been no direct assay to address σ^{70} release that would not involve a separative step (electrophoresis, chromatography, sedimentation, or washing) and that would distinguish between signals arising from active and inactive subpopulations of complexes (a serious problem, since in vitro only a fraction of complexes is competent to undergo transition to elongation [Levin et al., 1987; Kubori and Shimamoto, 1996]).

Here, we describe a method in which fluorescence resonance energy transfer (FRET; Lilley and Wilson, 2000) is used to monitor movement of a molecule relative to DNA, and we apply this method to distinguish between the σ^{70}-release and σ^{70}-nonrelease models. The method involves no separative step, and, since it involves detection of movement, is specifically sensitive to the active subpopulation of complexes (the subpopulation of complexes competent to undergo movement). The results obtained indicate that, in the majority of transcription complexes, σ^{70} is not released from RNAP upon transition from initiation to elongation, but, instead, remains associated with RNAP and translocates with RNAP.

Results and Discussion

FRET Assay for Movement Relative to DNA: Trailing-Edge FRET and Leading-Edge FRET

The method involves two complementary sets of experiments: (1) "trailing-edge-FRET" experiments, which monitor movement of a fluorescently labeled molecule relative to a fluorescent probe at the upstream end of DNA; and (2) "leading-edge-FRET" experiments, which monitor movement of a fluorescently labeled molecule

[1] Correspondence: ebright@mbcl.rutgers.edu
[2] These authors contributed equally to this work.
[3] Current address: Lawrence Berkeley National Laboratory, Berkeley, California 94720.

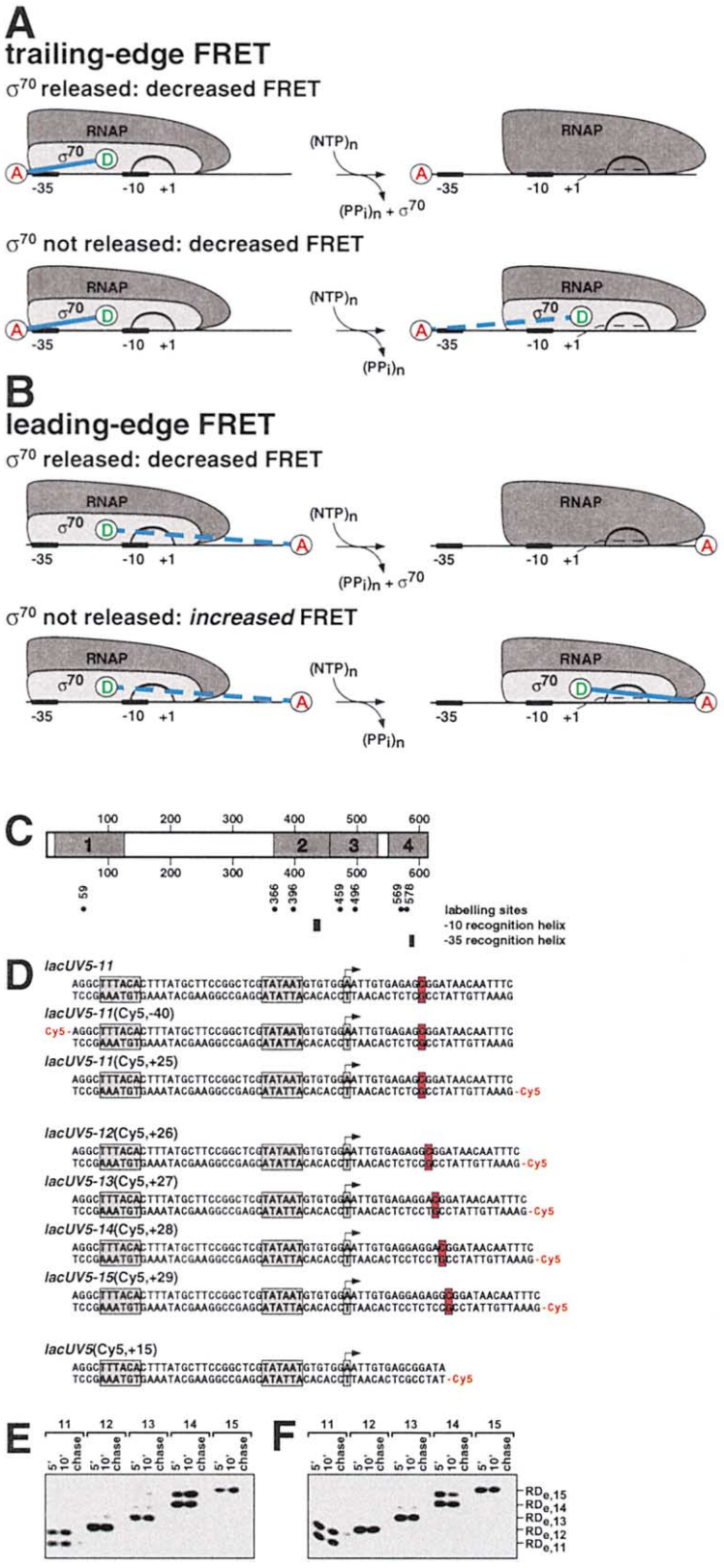

Figure 1. FRET Assay for Movement Relative to DNA

(A) Predictions of the σ^{70}-release (top) and σ^{70}-nonrelease (bottom) models with respect to a "trailing-edge-FRET" experiment in which a fluorescent donor (D) is incorporated within σ^{70}, and a fluorescent acceptor (A) is incorporated on upstream DNA.

(B) Predictions of the σ^{70}-release (top) and σ^{70}-nonrelease (bottom) models with respect to a "leading-edge-FRET" experiment in which a fluorescent donor (D) is incorporated within σ^{70}, and a fluorescent acceptor (A) is incorporated on downstream DNA.

(C) σ^{70} derivatives. Map of σ^{70} showing conserved regions 1–4 (shaded boxes; Gross et al., 1998), determinants for interaction with promoter −10 and −35 elements (solid bars; Gross et al., 1998), and sites at which fluorescent probe was incorporated (filled circles).

(D) DNA fragments. Top: DNA fragments used in analysis of $RD_{e,11}$ (*lacUV5* derivatives having no guanine residues on the template strand from +1 to +11, and having no fluorescent probe [as control], the fluorescent probe Cy5 at −40 [for trailing-edge FRET], or the fluorescent probe Cy5 at +25 [for leading-edge FRET]). Shaded boxes, transcription start site (with arrow), promoter −10 element, and promoter −35 element; red boxes, halt site. Middle: DNA fragments used in analysis of $RD_{e,12}$, $RD_{e,13}$, $RD_{e,14}$, and $RD_{e,15}$ (*lacUV5* derivatives having no guanine residues on the template strand from +1 to +12, +1 to +13, +1 to +14, or +1 to +15, and having Cy5 at +26, +27, +28, or +29). Bottom: DNA fragment used in analysis of reference construct having 100% σ^{70} occupancy and having Cy5 14 bp downstream of RNAP active center (*lacUV5* derivative having Cy5 at +15).

(E) Formation of $RD_{e,11}$, $RD_{e,12}$, $RD_{e,13}$, $RD_{e,14}$, and $RD_{e,15}$ upon addition of ApA, ATP, GTP, and UTP to RP_o, and ability to restart elongation ("chase") upon addition of CTP (experiments in gel matrix). Yields of $RD_{e,11}$ through $RD_{e,15}$ (determined by excision of bands and quantitation of RNA) were 0.6–0.7 mol RD_e per mol DNA, identical within error to the yield defined by in-gel trailing-edge FRET (0.64; Figure 2A). Formation of $RD_{e,n+1}$ is due to misincorporation at the halt site (0%–60%, depending on sequence context; see Krummel and Chamberlin, 1989; Metzger et al., 1993).

(F) As (E), but experiments in solution. Yields of $RD_{e,11}$ through $RD_{e,15}$ (determined by excision of bands and quantitation of RNA) were 0.6–0.8 mol RD_e per mol DNA, identical within error to the yield defined by in-solution trailing-edge FRET (0.65; Figure 2C).

relative to a fluorescent probe at the downstream end of DNA. The method detects movement as changes in distance between fluorescent probes and concomitant changes in efficiency of FRET (which is proportional to the inverse sixth power of distance between fluorescent probes [Lilley and Wilson, 2000]).

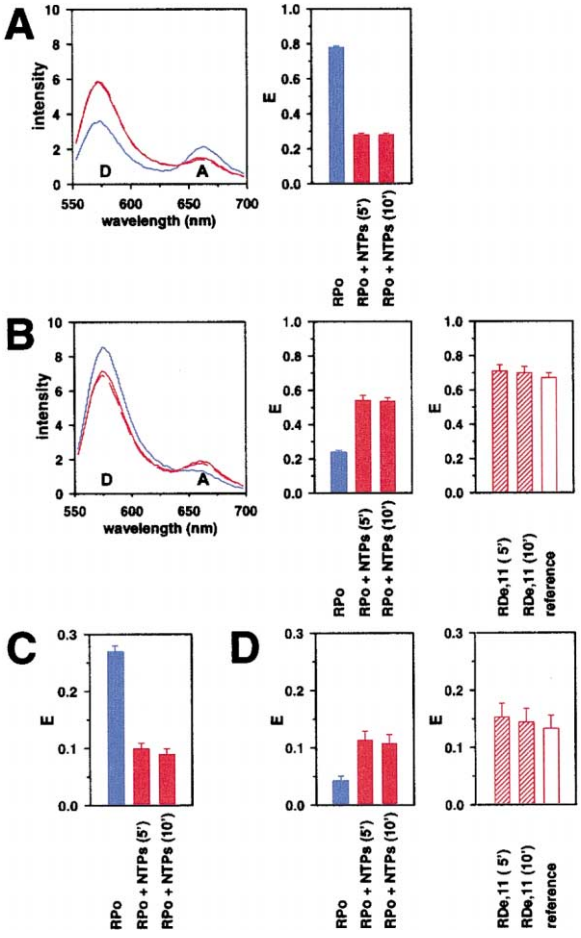

Figure 2. σ^{70} Translocates with RNAP

(A) Representative data for trailing-edge-FRET experiments assessing RP_o and $RD_{e,11}$ (data for experiments with σ^{70} derivative labeled at position 569 and DNA fragment *lacUV5-11*(Cy5,−40); experiments in gel matrix). Left panel: Blue line, fluorescence emission spectrum of RP_o; red line and red dashed line, fluorescence emission spectra 5 min and 10 min after addition of ApA, ATP, GTP, and UTP to RP_o. Right panel: Blue bars, FRET in RP_o; red bars, FRET 5 min and 10 min after addition of ApA, ATP, GTP, and UTP to RP_o.

(B) Representative data for leading-edge-FRET experiments assessing RP_o and $RD_{e,11}$ (data for experiments with σ^{70} derivative labeled at position 366 and DNA fragment *lacUV5-11*(Cy5,+25); experiments in gel matrix). Left panel: Blue line, fluorescence emission spectrum of RP_o; red solid and dashed lines, fluorescence emission spectra 5 min and 10 min after addition of ApA, ATP, GTP, and UTP to RP_o. Center panel: Blue bars, FRET in RP_o; red bars, FRET 5 min and 10 min after addition of ApA, ATP, GTP, and UTP to RP_o. Right panel: Red hatched bars, FRET in $RD_{e,11}$ (after correction for subpopulation of complexes not competent to undergo transition to elongation; see Experimental Procedures, equation 4); red open bar, FRET in reference construct having 100% σ^{70} occupancy and having Cy5 14 bp downstream of RNAP active center (RP_o with DNA fragment having Cy5 at +15).

(C) As (A), but experiments in solution.

(D) As (B), but experiments in solution.

Figure 1A shows the predictions of the σ^{70}-release and σ^{70}-nonrelease models with respect to a trailing-edge-FRET experiment in which a fluorescent probe, serving as donor, is incorporated at a single site within σ^{70}, and a second fluorescent probe, serving as acceptor, is incorporated at a single site on DNA upstream of the core promoter. In this case, the two models make identical predictions: upon transition to elongation, the probe-probe distance will increase, and FRET will decrease (due to, respectively, dissociation of σ^{70} from RNAP, or translocation of σ^{70} with RNAP).

Figure 1B shows the predictions of the σ^{70}-release and σ^{70}-nonrelease models with respect to a leading-edge-FRET experiment in which a fluorescent probe, serving as donor, is incorporated at a single site within σ^{70}, and a second fluorescent probe, serving as acceptor, is incorporated at a single site on DNA downstream of the core promoter. In this case, the two models make different predictions: According to the σ^{70}-release model, upon transition to elongation, the probe-probe distance will increase, and FRET will decrease (due to dissociation of σ^{70} from RNAP; Figure 1B, top panel). In contrast, according to the σ^{70}-nonrelease model, upon transition to elongation, the probe-probe distance will decrease, and FRET will increase (due to translocation of σ^{70} with RNAP; Figure 1B, bottom panel).

In this work, we have performed both trailing-edge-FRET and leading-edge-FRET experiments. The trailing-edge-FRET experiments have allowed us to establish that the transition to elongation occurs and to quantify the fraction of molecules competent to undergo the transition. The leading-edge-FRET experiments have allowed us to distinguish between the two models.

To incorporate fluorescent probe at single sites within σ^{70}, we prepared σ^{70} derivatives having single Cys residues at positions 59, 366, 396, 459, 496, 569, and 578 (see Owens et al., 1998; Callaci et al., 1998; Bown et al., 1999); we reacted each single-Cys σ^{70} derivative with tetramethylrhodamine maleimide under conditions that result in highly selective, highly efficient, derivatization of Cys; we reconstituted RNAP holoenzyme from each labeled σ^{70} derivative and RNAP; and we verified that each labeled RNAP holoenzyme derivative was functional in transcription (Figure 1C; Experimental Procedures, σ^{70} Derivatives; Experimental Procedures, RNAP Holoenzyme Derivatives). This yielded a set of seven fully functional labeled RNAP holoenzyme derivatives, each having tetramethylrhodamine incorporated at a single site within σ^{70}—with the sites spanning the length of σ^{70}, including σ^{70} regions 1, 2, 3, and 4 (Figure 1C).

To permit formation of defined elongation complexes, we prepared derivatives of the *lacUV5* promoter having the first template-strand guanine residue in the transcribed region at position +12, +13, +14, +15, or +16 (Figure 1D). With these DNA templates, upon formation of RP_o and addition of ApA, ATP, GTP, and UTP, RNAP initiates transcription, proceeds to position +11, +12, +13, +14, or +15, respectively, and halts (due to the absence of CTP, the next required NTP; Figures 1D–1F). The resulting halted complexes are bona fide elongation complexes; they are stable, they retain RNA, and they can be restarted upon addition of CTP (Figures 1E and 1F and data not shown). For trailing-edge-FRET experiments, we incorporated Cy5, serving as acceptor, immediately upstream of the core promoter, at position −40; for leading-edge-FRET experiments, we incorporated Cy5, serving as acceptor, downstream of the core promoter, at position +15, +25, +26, +27, +28, or +29 (Figure 1D).

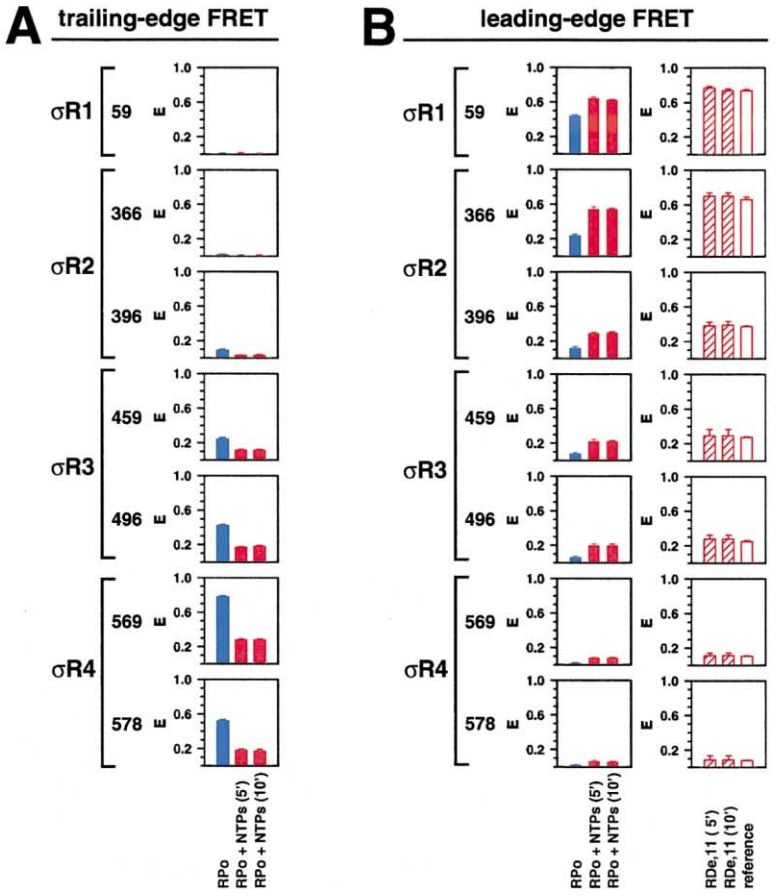

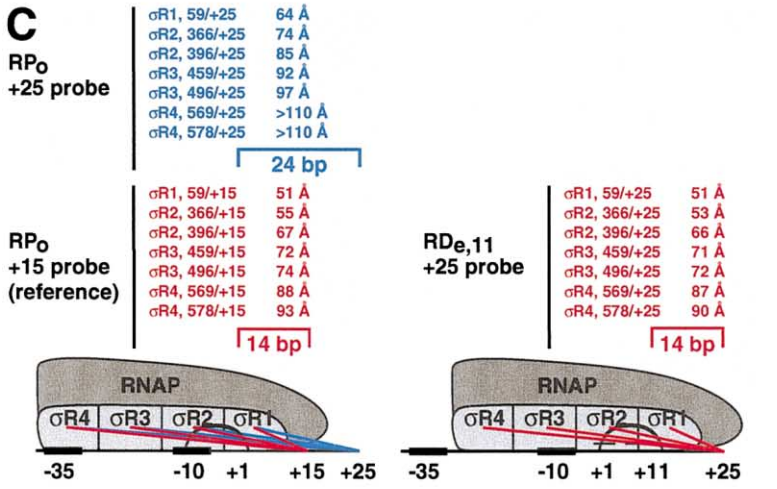

Figure 3. σ^{70} Translocates with RNAP as a Block, with Regions 1, 2, 3, and 4 Translocating in Concert

(A) Trailing-edge-FRET results for σ^{70} derivatives labeled at sites within regions 1, 2, 3, and 4 (DNA fragment *lacUV5-11*(Cy5,−40); experiments in gel matrix). Blue bars, FRET in RP_o; red bars, FRET 5 min and 10 min after addition of ApA, ATP, GTP, and UTP to RP_o.

(B) Leading-edge-FRET results for σ^{70} derivatives labeled at sites within regions 1, 2, 3, and 4 (DNA fragment *lacUV5-11*(Cy5,+25); experiments in gel matrix). Blue bars, FRET in RP_o; red filled bars, FRET 5 min and 10 min after addition of ApA, ATP, GTP, and UTP to RP_o; red hatched bars, FRET in $RD_{e,11}$ (after correction for subpopulation of complexes not competent to undergo transition to elongation; see Experimental Procedures, equation 4); red open bars, FRET in reference construct having 100% σ^{70} occupancy and having Cy5 14 bp downstream of RNAP active center (RP_o with DNA fragment having Cy5 at +15).

(C) Schematic interpretation of results. Probe-probe distances in RP_o (left) and $RD_{e,11}$(right) calculated from leading-edge-FRET results in (B) (see Experimental Procedures, equation 3). Blue at left, probe-probe distances in RP_o with Cy5 at +25 (Cy5 24 bp from RNAP active center); red at left, probe-probe distances in RP_o with Cy5 at +15 (reference construct; Cy5 14 bp from RNAP active center); red at right, probe-probe distances in $RD_{e,11}$ with Cy5 at +25 (Cy5 14 bp from RNAP active center). Within error, probe-probe distances are identical in RP_o with Cy5 at +15 (reference construct; red at left) and $RD_{e,11}$ with Cy5 at +25 (red at right).

(D) Structural interpretation of results. Positions of σ^{70} regions 1, 2, 3, and 4 in RP_o (left) and $RD_{e,11}$ (right). Positions of σ^{70} regions 1, 2, 3, and 4 are projected onto structural models of RP_o (Naryshkin et al., 2000; Ebright, 2000), and $RD_{e,11}$ (Korzheva et al., 2000), based on probe-probe distances in RP_o with Cy5 at +15 (reference construct; Cy5 14 bp from RNAP active center; distances in red in left panel of [C]) and in $RD_{e,11}$ with Cy5 at +25 (Cy5 14 bp from RNAP active center; distances in red in right panel of [C]). σ^{70} is in yellow; RNAP β′, β, α^I, and ω subunits are in orange, green, blue, and gray; DNA template and nontemplate strands are in gray and pink. The structure of the RNAP active-center cleft constrains the 14 bp DNA segment downstream of the RNAP active center—the DNA segment relevant to comparison of probe-probe distances in left and right panels—to be an unbent, straight B-form DNA duplex (Naryshkin et al., 2000; Korzheva et al., 2000; Ebright, 2000).

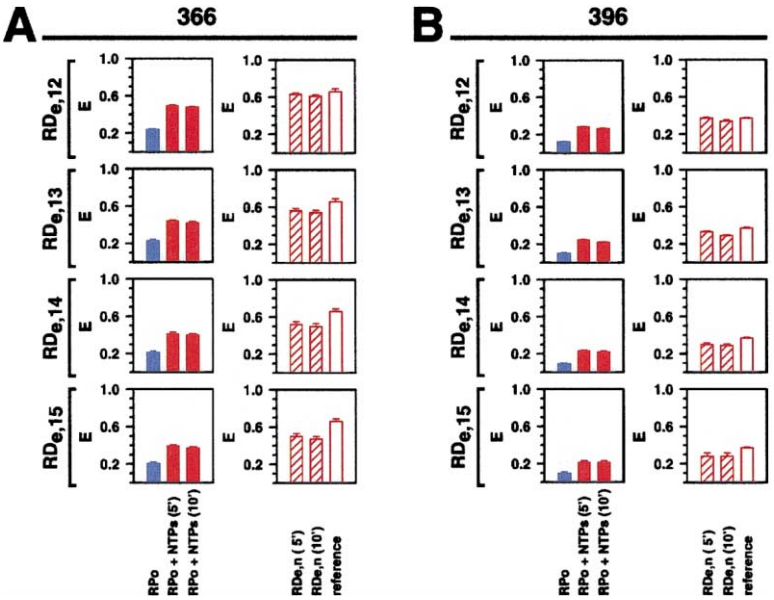

Figure 4. σ^{70} Translocates with RNAP upon, and after, Complete Filling of the RNA Exit Channel: $RD_{e,12}$, $RD_{e,13}$, $RD_{e,14}$, and $RD_{e,15}$

(A) Leading-edge-FRET results for $RD_{e,12}$, $RD_{e,13}$, $RD_{e,14}$, and $RD_{e,15}$ (data for experiments with σ^{70} derivative labeled at residue 366 and DNA fragments *lacUV5-12*(Cy5,+26) through *lacUV5-15*(Cy5,+29); experiments in gel matrix). Blue bars, FRET in RP_o; red filled bars, FRET 5 min and 10 min after addition of ApA, ATP, GTP, and UTP to RP_o; red hatched bars, FRET in $RD_{e,11}$ (after correction for subpopulation of complexes not competent to undergo transition to elongation; see Experimental Procedures, equation 4); red open bars, FRET in reference construct having 100% σ^{70} occupancy and having Cy5 14 bp downstream of RNAP active center (RP_o with DNA fragment having Cy5 at +15).

(B) As (A), but data for σ^{70} derivative labeled at residue 396.

To minimize complications due to fluorescence arising from free components, from aggregates of components, and from nonproductive complexes, we performed experiments using RP_o isolated by nondenaturing PAGE and analyzed in situ, in the gel matrix ("in-gel" FRET). Thus, we formed RP_o in solution; we challenged with heparin to disrupt nonspecific complexes (Cech and McClure, 1980); we isolated RP_o by nondenaturing PAGE; we located and excised the region of the gel containing RP_o; we mounted the excised gel slice in a cuvette and equilibrated in transcription buffer; and we measured fluorescence—in this manner obtaining data for RP_o. We then added ApA, ATP, GTP, and UTP directly to the cuvette, and, after defined intervals, again measured fluorescence—in this manner obtaining data for RD_e. The assumption that processes occurring in the gel matrix faithfully reflect processes in solution is supported by direct comparison of in-gel and in-solution FRET data (Figures 2A and 2B versus Figures 2C and 2D; see next section) and by the following: (1) Pores within the gel matrix (mean diameter $\approx$ 200 Å [Hsu and Cohen, 1984; Chui et al., 1995; Pluen et al., 1998]) are sufficiently large to accommodate RP_o or RD_e (diameter $\approx$ 150 Å [Naryshkin et al., 2000; Korzheva et al., 2000; Ebright, 2000]) and associated hydration. (2) Small molecules are able to diffuse within the gel matrix. (Upon addition of 0.1% SDS to cuvettes containing gel slices with labeled RP_o or RD_e, FRET is eliminated within 5 min at 37°C [J.M., A.K., V.M., E.K., and R.H.E., unpublished data].) (3) Macromolecules are able to diffuse within the gel matrix. [Confocal optical microscopy of gel slices containing labeled σ^{70}, RNAP, RP_o, or RD_e reveals three-dimensional Brownian walks spanning μm scale distances—which correspond to tens to hundreds of consecutive pores—on the subsecond to second time scale (diffusion rate = 1–10 $\mu m\ s^{-1}$; S. Weiss, A.K., and R.H.E., unpublished data).] (4) Transcription is able to occur within the gel matrix, and, at saturating NTP concentrations, occurs with yields and product distributions indistinguishable from those in solution (Figures 1E and 1F).

σ^{70} Translocates with RNAP

Representative data from trailing-edge-FRET experiments with RP_o and $RD_{e,11}$ are presented in Figure 2A (data for σ^{70} derivative labeled at residue 569, within σ^{70} region 4, and DNA fragment *lacUV5-11*(Cy5,−40) [Figures 1C and 1D]). Upon addition of the NTP subset that permits formation of an RNA product of 11 nt and incubation for 5 min, there is a 64% decrease in trailing-edge FRET, from 0.78 to 0.28 (Figure 2A, right panel). The residual trailing-edge FRET remains constant at 10 min (Figure 2A, right panel) and indeed after 30 min or longer (not shown). The residual trailing-edge FRET is attributable to the subpopulation of complexes not competent to undergo the transition to elongation (see quantitation of RNA yields indicating that, under these conditions, 60%–70% of complexes are competent to undergo the transition to elongation [Figure 1E]; see also Levin et al., 1987; Kubori and Shimamoto, 1996). Equivalent results are obtained with all σ^{70} derivatives labeled at sites sufficiently close to DNA position −40 to yield significant trailing-edge FRET in RP_o (i.e., σ^{70} derivatives labeled at one site in region 2, two sites in region 3, and two sites in region 4; Figures 1C and 3A). Equivalent results also are obtained with DNA fragments and/or NTP subsets permitting synthesis of longer RNA products (not shown). We conclude that, under our conditions, 64% of complexes are competent to undergo the transition to elongation, and that, in these complexes, σ^{70} leaves the promoter—either by dissociation (Figure 1A, top panel) or by translocation with RNAP (Figure 1A, bottom panel).

Representative data from leading-edge-FRET experiments with RP_o and $RD_{e,11}$ are presented in Figure 2B (data for σ^{70} derivative labeled at residue 366, within σ^{70} region 2, and DNA fragment *lacUV5-11*(Cy5,+25) [Figures 1C and 1D]). Upon addition of the NTP subset that permits formation of $RD_{e,11}$ and incubation for 5 min, there is a 2.3-fold increase in leading-edge FRET, from 0.24 to 0.54 (Figure 2B, center panel). Thus, molecules of σ^{70} that leave the promoter, as documented in the

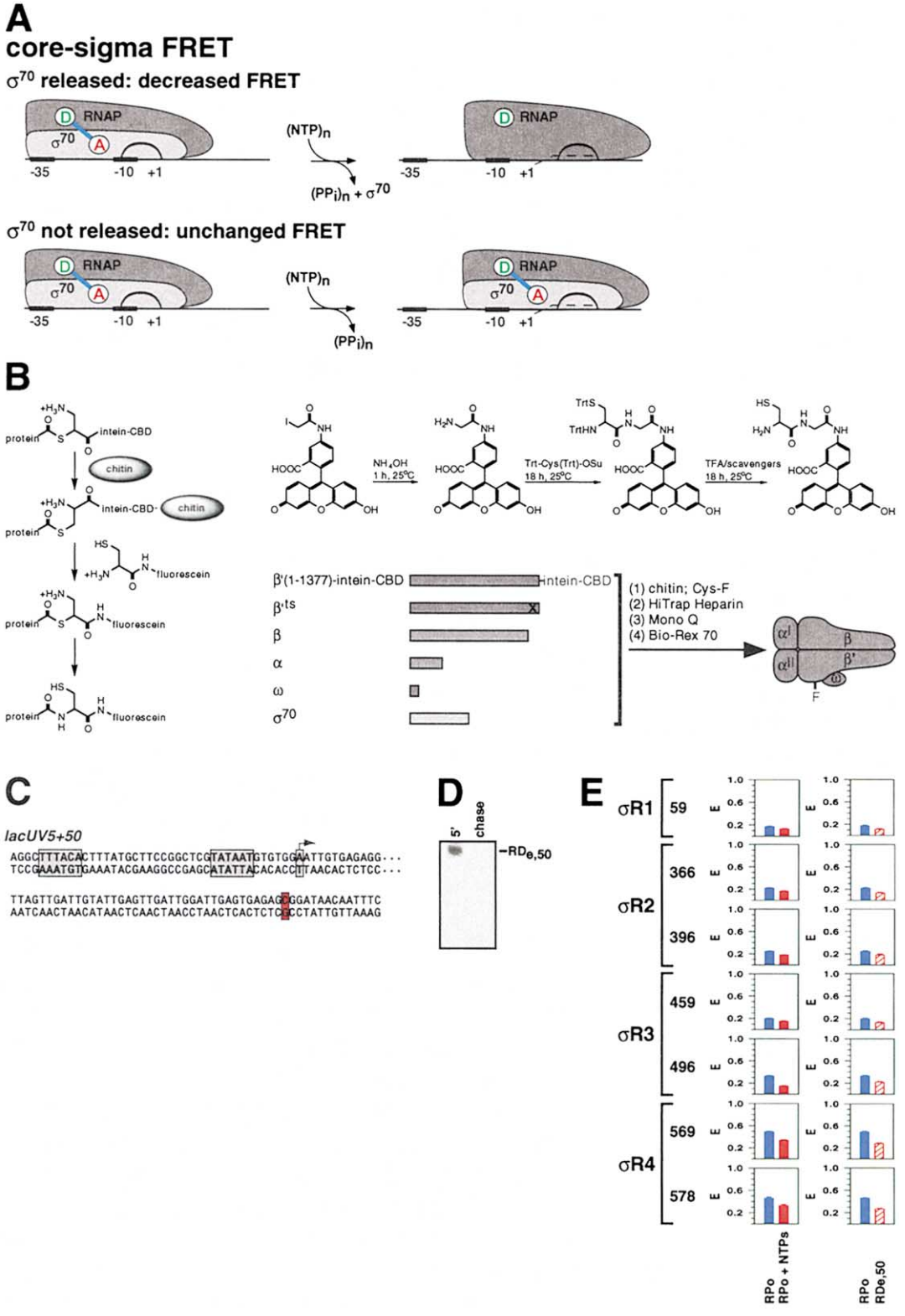

Figure 5. σ^{70} Translocates with RNAP upon, and after, Complete Filling of the RNA Exit Channel: $RD_{e,50}$

(A) Predictions of the σ^{70}-release (top) and σ^{70}-nonrelease (bottom) models with respect to a "core-σ^{70}-FRET" experiment in which a fluorescent donor (D) is incorporated within RNAP, and a fluorescent acceptor (A) is incorporated within σ^{70}.

(B) Labeling of RNAP (subunit composition $\beta'\beta\alpha^{I}\alpha^{II}\omega$). Left, intein-mediated C-terminal labeling with Cys-fluorescein (see Experimental Procedures, RNAP Derivatives; see also Chong et al., 1996,1997; Muir et al., 1998). Top right, synthesis of Cys-fluorescein. Bottom right, strategy for site-specific incorporation of fluorescein within intact, fully assembled, RNAP (at residue 1377 of β'). CBD, chitin binding domain; Cys-F, Cys-fluorescein.

trailing-edge FRET experiments (Figure 2A, right panel), arrive downstream (Figure 2B, center panel). Leading-edge FRET does not decrease after incubation for 10 min (Figure 2B, center panel) or indeed after incubation for 30 min or longer (not shown). Thus, molecules of σ^{70} arrive downstream, and they remain there, with a dissociation rate $<<10^{-3}\,s^{-1}$. These results are inconsistent with the σ^{70}-release model (Figure 1B, top panel), but are as predicted by the σ^{70}-nonrelease model (Figure 1B, bottom panel).

Correcting for the subpopulation of complexes not competent to undergo the transition to elongation, we calculate that leading-edge FRET in $RD_{e,11}$ is 0.70 (Figure 2B, right panel; see Experimental Procedures, equation 4). This value is 100% that measured for a reference construct having 100% σ^{70} occupancy and having the fluorescent acceptor the same distance downstream of the RNAP active center (i.e., RP_o with DNA fragment having the fluorescent acceptor at position +15; Figure 2B, right panel; Figures 3C and 3D). We conclude that 100% of molecules of $RD_{e,11}$ contain σ^{70}.

Equivalent results are obtained in experiments with a fully consensus promoter (*lacCONS*; derivative of *lacUV5* with single-base-pair substitution in −35 element and single-base-pair deletion in −35/−10 spacer) (not shown).

The experiments in Figures 2A and 2B were performed in a polyacrylamide gel matrix. To assess the possibility that the results reflect an artifact of having been performed in the gel matrix, we have performed analogous experiments in solution (Figures 2C and 2D). Experiments in solution yield lower apparent FRET, due to contamination of complexes by unbound DNA (which contains the fluorescent acceptor, but not the fluorescent donor, and which thus contributes to $F^{DA}_{665,620}$, but not to $F^{FRET}_{665,530}$; see Experimental Procedures, equation 2). Nevertheless, the results are clear—and are the same as in the gel matrix. In trailing-edge-FRET experiments in solution, there is a 65% decrease in FRET upon addition of NTPs (Figure 2C). In leading-edge-FRET experiments in solution, there is a 2.5-fold increase in FRET upon addition of NTPs (Figure 2D, left panel), and, after correction for the subpopulation not competent to undergo the transition to elongation, leading-edge FRET in $RD_{e,11}$ is calculated to be 100% that in the reference construct having 100% σ^{70} occupancy (Figure 2D, right panel). We conclude that in solution, as in the gel matrix, 100% of molecules of $RD_{e,11}$ contain σ^{70}.

σ^{70} Translocates with RNAP as a Block—with Regions 1, 2, 3, and 4 Translocating in Concert

The leading-edge FRET results in Figures 2B and 2D were obtained using a σ^{70} derivative labeled at a site within σ^{70} region 2 (the functional domain of σ^{70} responsible for recognition of the promoter −10 element [Figure 1C; Gross et al., 1998]). We have performed analogous experiments using σ^{70} derivatives labeled at each of six additional sites—sites spanning the length of σ^{70}, and including σ^{70} regions 1, 2, 3, and 4 (Figures 1C and 3B). In each case, equivalent leading-edge FRET results were obtained (Figures 1C and 3B). In each case, upon addition of the NTP subset that permits formation of $RD_{e,11}$, there was a large increase in leading-edge FRET (Figure 3B, left panel), and, after correction for the subpopulation not competent to undergo the transition to elongation, leading-edge FRET in $RD_{e,11}$ was calculated to be 100% that in the reference construct having 100% σ^{70} occupancy (Figure 3B, right panel). We conclude, in agreement with the results in the preceding section, that, in 100% of transcription complexes, σ^{70} remains associated with, and translocates with, RNAP upon transition to elongation. We conclude further that all four functional domains of σ^{70}—regions 1, 2, 3, and 4—translocate with RNAP.

From the efficiencies of leading-edge FRET in $RD_{e,11}$ (hatched red bars in Figure 3B), we have calculated the distances in $RD_{e,11}$ between probe sites in σ^{70} and the fluorescence acceptor on DNA at position +25, 14 bp downstream from the RNAP active center (red vectors and distances in Figure 3C, right panel; see Experimental Procedures, equation 3). Similarly, from the efficiencies of leading-edge FRET in the reference-construct RP_o (open red bars in Figure 3B), we have calculated the distances in the reference-construct RP_o between probe sites in σ^{70} and the fluorescence acceptor on DNA at position +15, 14 bp downstream from the RNAP active center (red vectors and distances in Figure 3C, left panel). For each probe site in σ^{70}, the distances in $RD_{e,11}$ and the reference-construct RP_o are identical, or nearly identical (red distances in Figure 3C, right panel vs. red distances in Figure 3C, left panel), suggesting that the orientations of σ^{70} relative to RNAP in $RD_{e,11}$ and the reference-construct RP_o are identical, or nearly identical—with σ^{70} region 1 located near the downstream half of the transcription bubble, σ^{70} region 2 located near the center and upstream half of the transcription bubble, and σ^{70} regions 3 and 4 located upstream of the transcription bubble (Figures 3C and 3D; see Naryshkin et al., 2000; Ebright, 2000). (Results of systematic protein-DNA photocrosslinking indicate that the 14 bp DNA segment downstream of the RNAP active center—the DNA segment relevant to this comparison of distances—is a straight B-form DNA duplex and is oriented relative to RNAP identically, or nearly identically, in RD_e and RP_o [Naryshkin et al., 2000; Korzheva et al., 2000; Ebright, 2000].) We conclude that σ^{70} translocates with RNAP

(C) DNA fragment used in analysis of $RD_{e,50}$ (*lacUV5* derivative having no guanine residues on the template strand from +1 to +50). Shaded boxes, transcription start site (with arrow), promoter −10 element, and promoter −35 element; red box, halt site.

(D) Formation of $RD_{e,50}$ upon addition of ApA, ATP, GTP, and UTP to RP_o, and ability to restart elongation ("chase") upon addition of CTP (experiments in gel matrix). The yield of $RD_{e,50}$ (determined by excision of bands and quantitation of RNA) was 0.71 mol $RD_{e,50}$ per mol DNA, identical to the yield defined in trailing-edge-FRET experiments with the same RNAP holoenzyme derivatives and DNA-template sequence (0.71; J.M. and R.H.E., unpublished data).

(E) Core-σ^{70}-FRET results for RP_o and $RD_{e,50}$ (data for experiments with σ^{70} derivatives labeled at residue 59, 366, 396, 459, 496, 569, or 578, and DNA fragment *lacUV5-50*; experiments in gel matrix). Blue filled bars, FRET in RP_o; red filled bars, FRET 5 min after addition of ApA, ATP, GTP, and UTP to RP_o; red hatched bars, FRET in $RD_{e,50}$ (after correction for subpopulation of complexes not competent to undergo transition to elongation; see Experimental Procedures, equation 5).

as a block—with regions 1, 2, 3, and 4 translocating in concert—and that σ^{70} maintains a constant, or nearly constant, spatial relationship with RNAP (Figures 3C and 3D).

σ^{70} Translocates with RNAP upon, and after, Complete Filling of the RNA Exit Channel

In $RD_{e,11}$, 9 nt of RNA are present as an RNA-DNA hybrid with the DNA template strand, and 2 nt of RNA are present within an RNA exit channel formed by RNAP—a channel that can accommodate 5 nt of RNA (Korzheva et al., 2000; Ebright, 2000). To assess effects of filling of the RNA exit channel on σ^{70} release, we have performed analogous leading-edge-FRET experiments using DNA fragments that permit formation of $RD_{e,12}$ (channel 3/5 full), $RD_{e,13}$ (channel 4/5 full), $RD_{e,14}$ (channel completely full), and $RD_{e,15}$ (channel completely full and 1 nt outside RNAP) (Figure 1D, center panel; Figure 4). Representative data are presented in Figure 4 (data for σ^{70} derivatives labeled at residues 366 and 396, within σ^{70} region 2). In each case, upon addition of NTPs, there is an in crease in leading-edge FRET (Figures 4A and 4B, left panels). Correcting for the subpopulation of complexes not competent to undergo transition to elongation, leading-edge FRET in $RD_{e,12}$, $RD_{e,13}$, $RD_{e,14}$, and $RD_{e,15}$ is estimated to be at least 90%, 80%, 80%, and 70%, respectively, that in the reference construct with 100% σ^{70} occupancy (Figures 4A and 4B, right panels) (with these estimates being minimal estimates, due to ability of $RD_{e,>11}$ to undergo reverse translocation ["backtracking"; see Komissarova and Kashlev, 1997; Nudler et al., 1997]). Experiments in solution yield equivalent results (not shown). We conclude that, in at least 70% of transcription complexes, σ^{70} is retained upon—and after—complete filling of the RNA exit channel.

Preliminary leading-edge-FRET experiments indicate retention of σ^{70} in $RD_{e,\geq 50}$ (J.M. and R.H.E., unpublished data). However, accurate quantitation of σ^{70} content in $RD_{e,\geq 50}$ by leading-edge FRET thus far has not been possible, due to the ability of $RD_{e,\geq 50}$ to undergo long-distance backtracking (J.M. and R.H.E., unpublished data; see Komissarova and Kashlev, 1997; Nudler et al., 1997).

To provide independent confirmation of retention of σ^{70} in $RD_{e,\geq 50}$, and to accurately quantify σ^{70} content in $RD_{e,\geq 50}$, we have analyzed FRET between a fluorescent probe incorporated on RNAP and a fluorescent probe incorporated on σ^{70} ("core-σ^{70}" FRET; Figure 5). For these experiments, we prepared RNAP holoenzyme derivatives having fluorescein (serving as donor) incorporated at residue 1377 of the β' subunit of RNAP and having tetramethylrhodamine (serving as acceptor) incorporated at residue 59, 366, 396, 459, 496, 569, or 578 of σ^{70} (Figures 5A and 5B). We then measured efficiencies of core-σ^{70} FRET in RP_o and $RD_{e,50}$ (Figures 5C–5E). The observed efficiencies of core-σ^{70} FRET after addition of the NTP subset that permits formation of $RD_{e,50}$ were 70%–76% that in RP_o (Figure 5E, left panels). Correcting for the subpopulation of complexes not competent to undergo the transition to elongation (29%—as measured in trailing-edge-FRET experiments with the same RNAP holoenzyme derivatives and DNA-template sequence [not shown], and by quantitation of moles of RNA synthesized per mole of DNA template [Figure 5D]), the efficiencies of core-σ^{70} FRET in $RD_{e,50}$ were 59%–67% that in RP_o (Figure 5E, right panels). Experiments in solution yield equivalent results (not shown). We conclude that, in $\sim$60% to $\sim$70% of transcription complexes, σ^{70} is retained even after synthesis of an RNA product 50 nt in length.

Physical isolation, using gentle separative methods, of $RD_{e,\geq 50}$ containing σ^{70} provides further independent confirmation of retention of σ^{70} even after synthesis of an RNA product 50 nt in length (Bar-Nahum and Nudler, 2001 [this issue of *Cell*]). (Bar-Nahum and Nudler detect σ^{70} in 6%–30% of molecules of $RD_{e,\geq 50}$. Since their assay involves separative steps, with attendant possible dissociation and loss of σ^{70} in separative steps, 6%–30% should be considered a lower bound.)

Prospect

Our results establish that, in the majority of transcription complexes, σ^{70} translocates with RNAP, σ^{70} translocates as a block—with regions 1, 2, 3, and 4 translocating in concert—and σ^{70} translocates upon, and after, complete filling of the RNA exit channel.

It remains to be determined whether a higher level of σ^{70} release occurs in more complex systems—i.e., in the presence of elongation, termination, and antitermination factors in vitro and in vivo (see, e.g., Greenblatt and Li, 1981; Gill et al., 1991). However, the present results establish that there is not an obligatory σ cycle in the experimental system in which the σ cycle was first defined—i.e., σ^{70} plus RNAP in vitro (Travers and Burgess, 1969; Hansen and McClure, 1980; Straney and Crothers, 1985; Krummel and Chamberlin, 1989; Metzger et al., 1993). More important, the present results establish that there is not an obligatory subunit-composition difference in the transcriptional machinery responsible for initiation and the transcriptional machinery responsible for elongation, and thus argue against the presumption that there are fundamental mechanistic differences in initiation and elongation.

We note that the trailing-edge-FRET/leading-edge-FRET method described in this report should be generalizable to permit analysis of movement of *any* molecule relative to *any* nucleic acid, and that straightforward extensions should permit kinetic analysis (by use of stopped-flow fluorescence spectroscopy; Lilley and Wilson, 2000; J.M. and R.H.E., unpublished data) and single-molecule kinetic analysis (by use of confocal optical microscopy; Lilley and Wilson, 2000; S. Weiss, A.K., and R.H.E., unpublished data).

Experimental Procedures

Plasmids

Plasmid pGEMD(−Cys), encoding a σ^{70} derivative with no Cys residues, and plasmids encoding σ^{70} derivatives with single Cys residues at positions 59, 366, 396, 459, and 496 were described in Owens et al., 1998; Callaci et al., 1998; and Bown et al., 1999. Plasmids encoding σ^{70} derivatives with single Cys residues at positions 569 and 578 were constructed using site-directed mutagenesis (methods as in Sambrook and Russell, 2001). Plasmid pVMβ'1377-IC encodes a three-part fusion protein, consisting of β'(1–1377), followed by a modified *Saccharomyces cerevisiae* VMA-I intein, followed by a chitin binding domain (CBD). Plasmid pVMβ'1377-IC was constructed by replacement of the XhoI-StuI segment of plasmid pRL663 (Wang et al., 1995) by a XhoI-StuI DNA fragment carrying the coding se-

quence for intein-CBD (generated by add-on-PCR using plasmid pCYB2 [Chong et al., 1997] as template), followed by use of site-directed-mutagenesis (methods as in Sambrook and Russell, 2001) to fuse coding sequences for β'(1–1377) and intein-CBD (fusion junction = β'^{1377}-Pro-Gly-intein[1]).

σ^{70} Derivatives

Unlabeled σ^{70} and σ^{70} derivatives were prepared essentially as in Callaci et al., 1998, but using chromatography on Mono-Q (Amersham-Pharmacia Biotech, Inc.) in place of chromatography on DE52. Labeled σ^{70} derivatives were prepared using Cys-specific chemical modification (Figure 1C). Reaction mixtures for labeling of σ^{70} contained (1 ml): 20 μM single-Cys σ^{70} derivative (subjected to solid-phase reduction on Reduce-Imm [Pierce, Inc.] per manufacturer's instructions immediately before use), 200 μM tetramethylrhodamine-5-maleimide (Molecular Probes, Inc.), 100 mM sodium phosphate (pH 8.0), and 1 mM EDTA. Following 1 hr on ice, products were purified by gel-filtration chromatography on Bio-Gel P6DG (Bio-Rad, Inc.), and stored in 20 mM Tris-HCl (pH 7.9), 100 mM NaCl, 0.1 mM EDTA, 0.1 mM DTT, and 50% glycerol at −20°C. Efficiencies of labeling, determined by measurement of UV-absorbance, were ~90%; site-specificities of labeling, determined by comparison to products of control reactions with Cys-free σ^{70} derivative, were ~90%.

RNAP Derivatives

Unlabeled RNAP was prepared essentially as in Niu et al., 1996. Labeled RNAP—with fluorescein incorporated at residue 1377 of β'—was prepared by intein-mediated C-terminal labeling (Figure 5B; see also Chong et al., 1996, 1997; Muir et al., 1998). The procedure involved: (1) coexpression of genes encoding β'(1–1377)-intein-CBD, β'^{ts397c} (temperature-sensitive, assembly-defective β' derivative [Christie et al., 1996; Minakhin et al., 2001]), β, α, ω, and σ^{70}; (2) affinity-capture of RNAP holoenzyme containing β'(1–1377)-intein-CBD on chitin; (3) cleavage, elution, and concurrent labeling with Cys-fluorescein; and (4) removal of σ^{70}. Cultures of strain 397c (*rpoC397 argG thi lac* ($\lambda cI_{857}h_{80}S_{168}d$*lac*$^+$) [Christie et al., 1996]) transformed with plasmid pVMβ'1377-IC were shaken in 1 liter 4× LB containing 170 mM NaCl, 3 mM IPTG, and 200 μg/ml ampicillin, at 37°C until OD_{600} = 1.5, and were harvested by centrifugation (5000 × g; 15 min at 4°C). Cell lysis, Polymin P precipitation, and ammonium sulfate precipitation were performed as in Burgess and Jendrisak, 1975, except that 5 ml protease-inhibitor mixture P8465 (Sigma, Inc.) was included in the lysis buffer, and 1 ml 0.8 mM σ^{70} was added immediately after lysis. Samples were suspended in 25 ml buffer A (20 mM Tris-HCl [pH 7.9], 0.1 mM EDTA, and 5% glycerol) containing 100 mM NaCl, and applied to a 10 ml column of chitin (New England Biolabs, Inc.) in buffer A containing 100 mM NaCl. The column was washed with 50 ml buffer A containing 500 mM NaCl, washed with 25 ml buffer B (20 mM sodium phosphate [pH 7.3], 200 mM NaCl, and 0.5 mM Tris[2-carboxyethyl]phosphine [TCEP; Pierce, Inc.]), and equilibrated with 10 ml buffer B containing 150 μM Cys-fluorescein (summary of synthesis in Figure 5B, top right; details of synthesis to be presented elsewhere), 0.5% (v/v; saturating) thiophenol, and 0.1 mM phenylmethysulfonyl fluoride. Following 8 hr at 4°C, 10–20 ml buffer A containing 200 mM NaCl and 0.1 mM DTT was applied to the column, and 1 ml fractions were collected. Fractions containing labeled RNAP holoenzyme were pooled, centrifuged to remove fine-particulate chitin (15000 × g; 15 min at 4°C); filtered through 50 ml Sephadex LH-20 (Amersham-Pharmacia Biotech, Inc.) in buffer A containing 200 mM NaCl and 0.1 mM DTT to remove excess Cys-fluorescein; and chromatographed on HiTrap heparin (Amersham-Pharmacia Biotech, Inc.), Mono-Q (Amersham-Pharmacia Biotech, Inc.), and Bio-Rex70 (Bio-Rad, Inc.), essentially as in Kashlev et al. (1996), to remove σ^{70}. Labeled RNAP was dialyzed into 40 mM Tris-HCl (pH 7.9), 200 mM NaCl, 0.1 mM EDTA, 0.5 mM TCEP, and 50% glycerol, and was stored at −20°C. Yields were ~0.1 mg; efficiencies of labeling, determined by measurement of UV absorbance, were ≥95%; site-specificities of labeling, determined by comparison to products of control reactions with RNAP derivatives not containing intein-CBD and with RNAP derivatives containing intein-CBD fused to subunits other than β', were ≥95%.

RNAP Holoenzyme Derivatives

RNAP holoenzyme derivatives were prepared by incubation of 1 μM RNAP or RNAP derivative with 2 μM σ^{70} derivative (1 μM σ^{70} derivative for in-solution experiments) in 20 μl transcription buffer (TB: 50 mM Tris-HCl [pH 8.0], 100 mM KCl, 10 mM $MgCl_2$, 1 mM dithiothreitol, 10 μg/ml bovine serum albumin, and 5% glycerol) for 20 min at 25°C. Transcriptional activities of labeled RNAP holoenzyme derivatives (determined as in Suh et al., 1992) were indistinguishable from those of unlabeled RNAP holoenzyme.

DNA Fragments

Oligodeoxyribonucleotides were prepared by automated β-cyanoethyl-phosphoramidite synthesis; Cy5 was incorporated using Cy5-CE Phosphoramidite (Glen Research, Inc.). DNA fragments were prepared by PCR with synthetic primers and templates and were purified by PAGE essentially as in Sambrook and Russell, 2001.

RP_o: in-Gel

Reaction mixtures contained (20 μl): 200 nM RNAP holoenzyme derivative and 50 nM DNA fragment in TB. Following 15 min at 37°C, 0.5 μl 1 mg/ml heparin was added (to disrupt nonspecific complexes [Cech and McClure, 1980]), and, following a further 5 min at 37°C, reaction mixtures were applied to 5% polyacrylamide slab gels (30:1 acrylamide/bisacrylamide; 6 × 9 × 0.1 cm) and electrophoresed in 90 mM Tris-borate (pH 8.0) and 0.2 mM EDTA (20 V/cm; 30 min at 37°C). Gel regions containing RP_o were identified using an x/y fluorescence scanner (Storm 860; Molecular Dynamics, Inc.) and excised.

RP_o: in-Solution

Reaction mixtures contained (20 μl): 200 nM RNAP holoenzyme derivative and 50 nM DNA fragment in TB. Following 15 min at 37°C, 0.5 μl 1 mg/ml heparin-Sepharose (Amersham-Pharmacia Biotech, Inc.) was added (to disrupt nonspecific complexes and to remove free RNAP holoenzyme [Cech and McClure, 1980]), and, following a further 5 min at 37°C, samples were centrifuged, and supernatants were transferred to new tubes.

Analysis of RNA: in-Gel

Gel slices containing RP_o were transferred to a microcentrifuge tube containing 45 μl TB and equilibrated 5 min at 37°C. RNA synthesis was initiated in situ, in the gel matrix, by addition of 5 μl 5 mM ApA, 1 mM ATP, 1 mM GTP, and 1 mM [α-^{32}P]UTP (10 Bq/fmol). Following 0, 5, or 10 min at 37°C, reactions were terminated by addition of 20 μl 80% formamide, 10 mM EDTA, 0.04% bromophenol blue, and 0.04% xylene cyanol (or, in experiments with a chase, reaction mixtures were supplemented with 1 μl 25 mM ATP, 25 mM CTP, 25 mM GTP, and 25 mM UTP, incubated an additional 10 min at 37°C, and then terminated). Products were heated 30 min at 90°C and were analyzed by urea-PAGE (Sambrook and Russell, 2001) and PhosphorImaging.

Analysis of RNA: in-Solution

Experiments were performed as in the preceding section, except that RP_o was prepared in solution, and final NTP concentrations were 12.5 μM in primary reactions and 60 μM in chase reactions.

Trailing-Edge FRET and Leading-Edge FRET: in-Gel

Gel slices containing RP_o prepared from labeled RNAP holoenzyme and labeled DNA (donor-acceptor experiment, DA), from labeled RNAP holoenzyme and unlabeled DNA (donor-only control, D), and from unlabeled RNAP holoenzyme and labeled DNA (acceptor-only control, A), were mounted in submicro fluorometer cuvettes (Starna Inc.; catalog number 26.40f-Q-10) containing 92 μl TB. For each gel slice, fluorescence emission intensities (excitation wavelengths = 530 nm and 620 nm; excitation and emission slit widths = 5 nm; QuantaMaster QM1/SE901/SE910Q or QM1/SE901/SE920Q; PTI, Inc.) were measured after incubation for 5 min at 37°C (data labeled "RP_o" in figures) and were again measured after addition of 8 μl 6 mM ApA, 1.25 mM ATP, 1.25 mM GTP, and 1.25 mM UTP, and incubation for 5 min and 10 min at 37°C (data labeled "RP_o + NTPs" in figures). Fluorescence emission intensities were corrected for background by subtraction of fluorescence emission intensities for equivalent-size gel slices not containing RP_o. The fluorescence emission intensity attributable to FRET ($F^{FRET}_{665,530}$), the efficiency of FRET (E), and the donor-acceptor distance (r) were calculated as

follows (see Clegg, 1992; Lilley and Wilson, 2000):

$$F^{FRET}_{665,530} = F^{DA}_{665,530} - \frac{F^{DA}_{580,530} \cdot F^{D}_{665,530}}{F^{D}_{580,530}} - \frac{F^{DA}_{665,620} \cdot F^{A}_{665,530}}{F^{A}_{665,620}} \quad (1)$$

$$E = \frac{F^{FRET}_{665,530} \cdot \epsilon^{A}_{620}}{F^{DA}_{665,620} \cdot \epsilon^{D}_{530} \cdot d} \quad (2)$$

$$r = r_o[(1/E) - 1]^{1/6} \quad (3)$$

where d is the efficiency of labeling of the σ^{70} derivative (0.8–1 in these experiments; see Experimental Procedures, σ^{70} Derivatives), and where ϵ^{D}_{530} = 42,600 M^{-1} cm^{-1}, ϵ^{A}_{620} = 110,000 M^{-1} cm^{-1}, and r_o = 61 Å.

The efficiency of leading-edge FRET within RD_e, E_{RDe}, was calculated as:

$$E_{RDe} = [E_{RPo+NTPs} - (1 - f)E_{RPo}]/f \quad (4)$$

where f is the fraction of molecules competent to undergo the transition to elongation (0.64–0.65 in these experiments; Figures 2A and 2C).

Trailing-Edge FRET and Leading-Edge FRET: in-Solution

Experiments were performed as in the preceding section, except that RP_o was prepared in solution, and final NTP concentrations were 12.5 μM.

Core-σ^{70} FRET: in-Gel

In-gel core-σ^{70}-FRET experiments were performed analogously to in-gel trailing-edge-FRET and leading-edge-FRET experiments. Excitation was at 470 nm and 540 nm; emission was monitored at 520 nm and 580 nm. Fluorescence emission intensities attributable to FRET and efficiencies of FRET were calculated using equations 1 and 2 (substituting 530, 620, 580, and 665, by 470, 540, 520, and 580, respectively) and using d = 0.95–1 (see Experimental Procedures, RNAP Holoenzyme Derivatives), ϵ^{D}_{470} = 26,600 M^{-1} cm^{-1}, and ϵ^{A}_{540} = 52,000 M^{-1} cm^{-1}. The efficiency of core-σ^{70} FRET within $RD_{e,50}$, $E_{RDe,50}$, was calculated as:

$$E_{RDe,50} = [E_{RPo+NTPs} - (1 - f)E_{RPo}]/f \quad (5)$$

where f is the fraction of molecules competent to undergo the transition to elongation (0.71 in these experiments; Figure 5D).

Core-σ^{70} FRET: in-Solution

Experiments were performed as in the preceding section, except that RP_o was prepared in solution, and final NTP concentrations were 12.5 μM.

Acknowledgments

We thank W. Niu for assistance in development of procedures for labeling of β′; S. Busby, T. Heyduk, C. Meares, and R. Landick for plasmids; and G. Bar-Nahum, E. Nudler, and S. Weiss for discussion. This work was supported by NIH grant GM41376 and a Howard Hughes Medical Institute Investigatorship to R.H.E.

Received May 30, 2001; revised July 16, 2001.

References

Bar-Nahum, G., and Nudler, E. (2001). Isolation and characterization of σ^{70}-retaining transcription elongation complexes from *Escherichia coli*. Cell *106*, this issue, 443–451.

Bown, J., Owens, J., Meares, C., Fujita, N., Ishihama, A., Busby, S., and Minchin, S. (1999). Organization of open complexes at *Escherichia coli* promoters. J. Biol. Chem. *274*, 2263–2270.

Burgess, R., and Jendrisak, J. (1975). A procedure for the rapid, large-scale purification of Escherichia coli DNA-dependent RNA polymerase involving Polymin P precipitation and DNA-cellulose chromatography. Biochemistry *14*, 4634–4638.

Callaci, S., Heyduk, E., and Heyduk, T. (1998). Conformational changes of *Escherichia coli* RNA polymerase σ^{70} factor induced by binding to the core enzyme. J. Biol. Chem. *273*, 32995–33001.

Carpousis, A., and Gralla, J. (1985). Interaction of RNA polymerase with *lac*UV5 promoter DNA during mRNA initiation and elongation. J. Mol. Biol. *183*, 165–177.

Cech, C., and McClure, W. (1980). Characterization of ribonucleic acid polymerase-T7 promoter binary complexes. Biochemistry *19*, 2440–2447.

Chong, S., Shao, Y., Paulus, H., Benner, J., Perler, F., and Xu, M.-Q. (1996). Protein splicing involving the *Saccharomyces cerevisiae* VMA intein. J. Biol. Chem. *271*, 22159–22168.

Chong, S., Mersha, F., Comb, D., Scott, M., Landry, D., Vence, L., Perler, F., Benner, J., Kucera, R., Hirvonen, C., et al. (1997). Single-column purification of free recombinant proteins using a self-cleavable affinity tag derived from a protein splicing element. Gene *192*, 271–281.

Christie, G., Cale, S., Isaksson, L., Jin, D., Xu, M., Sauer, B., and Calendar, R. (1996). Escherichia coli rpoC397 encodes a temperature-sensitive C-terminal frameshift in the β′ subunit of RNA polymerase that blocks growth of bacteriophage P2. J. Bacteriol. *178*, 6991–6993.

Chui, M., Phillips, R.J., and McCarthy, M. (1995). Measurement of the porous microstructure of hydrogels by nuclear magnetic resonance. J. Colloid Interface Science *174*, 336–344.

Clegg, R. (1992). Fluorescence resonance energy transfer and nucleic acids. Methods Enzymol. *211*, 353–388.

Daube, S., and von Hippel, P. (1999). Interactions of *Escherichia coli* σ^{70} within the transcription elongation complex. Proc. Natl. Acad. Sci. USA *96*, 8390–8395.

Ebright, R. (2000). RNA polymerase: structural similarities between bacterial RNA polymerase and eukaryotic RNA polymerase II. J. Mol. Biol. *304*, 687–689.

Gill, S., Weitzel, S., and von Hippel, P. (1991). *Escherichia coli* σ^{70} and NusA proteins: I. Binding interactions with core RNA polymerase in solution and within the transcription complex. J. Mol. Biol. *220*, 307–324.

Greenblatt, J., and Li, J. (1981). Interaction of the sigma factor and the *nusA* gene protein of E. coli with RNA polymerase in the initiation-termination cycle of transcription. Cell *24*, 421–428.

Gross, C., Chan, C., Dombroski, A., Gruber, T., Sharp, M., Tupy, J., and Young, B. (1998). The functional and regulatory roles of sigma factors in transcription. Cold Spring Harbor Symp. Quant. Biol. *63*, 141–155.

Hansen, U., and McClure, W. (1980). Role of the σ^{70} subunit of *Escherichia coli* RNA polymerase in initiation. II. Release of σ^{70} from ternary complexes. J. Biol. Chem. *255*, 9564–9570.

Hsu, T.-P., and Cohen, C. (1984). Observations on the structure of a polyacrylamide gel from electron micrographs. Polymer *25*, 1419–1423.

Kashlev, M., Nudler, E., Severinov, K., Borukhov, S., Komissarova, N., and Goldfarb, A. (1996). Histidine-tagged RNA polymerase of *Escherichia coli* and transcription in solid phase. Methods Enzymol. *274*, 326–334.

Komissarova, N., and Kashlev, M. (1997). Transcriptional arrest: *Escherichia coli* RNA polymerase translocates backward, leaving the 3′ end of the RNA intact and extruded. Proc. Natl. Acad. Sci. USA *94*, 1755–1760.

Korzheva, N., Mustaev, A., Kozlov, M., Malhotra, A., Nikiforov, V., Goldfarb, A., and Darst, S. (2000). A structural model of transcription elongation. Science *289*, 619–625.

Krummel, B., and Chamberlin, M. (1989). RNA chain initiation by *Escherichia coli* RNA polymerase. Structural transitions of the enzyme in early ternary complexes. Biochem *28*, 7829–7842.

Kubori, T., and Shimamoto, N. (1996). A branched pathway in the early stage of transcription by *Escherichia coli* RNA polymerase. J. Mol. Biol. *256*, 449–457.

Levin, J., Krummel, B., and Chamberlin, M. (1987). Isolation and properties of transcribing ternary complexes of *Escherichia coli* RNA polymerase positioned at a single template base. J. Mol. Biol. *196*, 85–100.

Lilley, D.M.J., and Wilson, T. (2000). Fluorescence resonance energy

transfer as a structural; tool for nucleic acids. Curr. Opin. Chem. Biol. *4*, 507–517.

Minakhin, L., Bhagat, S., Brunning, A., Campbell, E., Darst, S., Ebright, R., and Severinov, K. (2001). Bacterial RNA polymerase subunit omega and eukaryotic RNA polymerase subunit RPB6 are sequence, structural, and functional homologs and promote RNA polymerase assembly. Proc. Natl. Acad. Sci. USA *98*, 892–897.

Muir, T., Sondhi, D., and Cole, P. (1998). Expressed protein ligation: a general method for protein engineering. Proc. Natl. Acad. Sci. USA *95*, 6705–6710.

Naryshkin, N., Revyakin, A., Kim, Y., Mekler, V., and Ebright, R. (2000). Structural organization of the RNA polymerase-promoter open complex. Cell *101*, 601–611.

Niu, W., Kim, Y., Tau, G., Heyduk, T., and Ebright, R. (1996). Transcription activation at Class II CAP-dependent promoters: two interactions between CAP and RNA polymerase. Cell *87*, 1123–1134.

Nudler, E., Mustaev, A., Lukhtanov, E., and Goldfarb, A. (1997). The RNA-DNA hybrid maintains the register of transcription by preventing backtracking of RNA polymerase. Cell *89*, 33–41.

Osumi-Davis, P., Woody, A., and Woody, R. (1987). Transcription initiation by Escherichia coli RNA polymerase at the gene II promoter of M13 phage: stability of ternary complex, direct photocrosslinking to nascent RNA, and retention of sigma subunit. Biochim. Biophys. Acta *910*, 130–141.

Owens, J., Miyake, R., Murakami, K., Chmura, A., Fujita, N., Ishihama, A., and Meares, C. (1998). Mapping the σ^{70} subunit contact sites on *Escherichia coli* RNA polymerase with a σ^{70}-conjugated chemical protease. Proc. Natl. Acad. Sci. *95*, 6021–6026.

Pluen, A., Tinland, B., Sturm, J., and Weill, G. (1998). Migration of single-stranded DNA in polyacrylamide gels during electrophoresis. Electrophoresis *19*, 1548–1559.

Ring, B.Z., Yarnell, W., and Roberts, J. (1996). Function of E. coli RNA polymerase σ factor σ^{70} in promoter-proximal pausing. Cell *86*, 485–493.

Sambrook, J., and Russell, D. (2001). Molecular Cloning: A Laboratory Manual (Cold Spring Harbor, NY: Cold Spring Harbor Laboratory Press).

Shimamoto, N., Kamigochi, T., and Utiyama, H. (1986). Release of the σ subunit of *Escherichia coli* DNA-dependent RNA polymerase depends mainly of time elapsed after the start of initiation, not in length of product RNA. J. Biol. Chem. *261*, 11859–11865.

Straney, D., and Crothers, D. (1985). Intermediates in transcription initiation from the E. coli lac UV5 promoter. Cell *43*, 449–459.

Straney, D., and Crothers, D. (1987). A stressed intermediate in the formation of stably initiated RNA chains at the *Escherichia coli lac* UV5 promoter. J. Mol. Biol. *193*, 267–278.

Suh, W., Leirmo, S., and Record, M.T. (1992). Roles of Mg^{2+} in the mechanism of formation and dissociation of open complexes between Escherichia coli RNA polymerase and the lambda PR promoter: kinetic evidence for a second open complex requiring Mg^{2+}. Biochemistry *31*, 7815–7825.

Travers, A., and Burgess, R. (1969). Cyclic re-use of the RNA polymerase sigma factor. Nature *222*, 537–540.

Wang, D., Meier, T., Chan, C., Feng, G., Lee, D., and Landick, R. (1995). Discontinuous movements of DNA and RNA in RNA polymerase accompany formation of a paused transcription complex. Cell *81*, 341–350.